Preprint
UCRL-JC-148209

Prediction of Carbon Monoxide and Hydrocarbon Emissions in Isooctane HCCI Engine Combustion Using Multi-Zone Simulations

D.L. Flowers, S.M. Aceves, J. Martinez-Frias, R.W. Dibble

This article was submitted to
29th International Symposium on Combustion, Sapporo, Japan, July 21-26, 2002

May 2, 2002

U.S. Department of Energy
Lawrence Livermore National Laboratory

Paper ID: flowersd18364
Publications Number: 2c13

Prediction of Carbon Monoxide and Hydrocarbon Emissions in Isooctane HCCI Engine Combustion Using Multi-Zone Simulations

Daniel L. Flowers, Salvador M. Aceves, Joel Martinez-Frias
Lawrence Livermore National Laboratory

Robert W. Dibble
University of California - Berkeley

Abstract

Homogeneous Charge Compression Ignitions (HCCI) engines show promise as an alternative to Diesel engines, yet research remains: development of practical HCCI engines will be aided greatly by accurate modeling tools. A novel detailed chemical kinetic model that incorporates information from a computational fluid mechanics code has been developed to simulate HCCI combustion. This model very accurately predicts many aspects of the HCCI combustion process. High-resolution computational grids can be used for the fluid mechanics portion of the simulation, but the chemical kinetics portion of the simulation can be reduced to a handful of computational zones (for all previous work 10 zones have been used). While overall this model has demonstrated a very good predictive capability for HCCI combustion, previous simulations using this model have tended to underpredict carbon monoxide emissions by an order of magnitude. A factor in the underprediction of carbon monoxide may be that all previous simulations have been conducted with 10 chemical kinetic zones. The chemistry that results in carbon monoxide emissions is very sensitive to small changes in temperature within the engine. The resolution in temperature is determined directly by the number of zones. This paper investigates how the number of zones (i.e. temperature resolution) affects the model's prediction of hydrocarbon and carbon monoxide emissions in an HCCI engine. Simulations with 10, 20, and 40 chemical kinetic zones have been conducted using a detailed chemical kinetic mechanism (859 species, 3606 reactions) to simulate an isooctane fueled HCCI engine. The results show that 10-zones are adequate to resolve the hydrocarbon emissions, but a greater numbers of zones are required to resolve carbon monoxide emissions. Results are also presented that explore spatial sources of the exhaust emissions within the HCCI engine combustion chamber.

Introduction

The Homogeneous Charge Compression Ignition (HCCI) engine is being considered as a potential alternative to Diesel engines. The main advantage of this process is that peak combustion temperatures are low yielding very low oxides of nitrogen (NO_x) emissions – without the need for catalytic reduction [1-6]. For broader background on current HCCI research the reader is directed to recent technical papers; the most comprehensive source of these would likely be several special publications from the Society of Automotive Engineers [7-9]. The common conceptual description of the HCCI engine is that ignition of a premixture of fuel and air occurs due to the compression process in a piston engine. Combustion in an HCCI engine cycle has been hypothetically described as simultaneous multipoint autoignition; heat release would therefore not be controlled by flame propagation (as in a spark-ignited engine) or fuel-air mixing (as in a Diesel). This global autoignition is thought to initiate when the fuel-air mixture is subjected to certain temperature and pressure time histories during the engine cycle. The timing of combustion occurs based on the interaction of the chemical processes with the temperature and pressure histories. Unlike the combustion in spark-ignition or diesel engines, turbulent mixing has little effect on the heat release process in HCCI combustion. Spectroscopic and imaging investigations of HCCI verify that simultaneous multi-point ignition occurs with no flame propagation [10-14], supporting the hypothesis that heat release in dominated by chemical kinetics.

A simulation method has been developed that takes advantage of the description that the chemical heat release process in an HCCI engine occurs independent of flame

propagation or fuel-air mixing. Instead of attempting to directly link a fluid mechanics code with a chemical kinetics code, an alternative, sequential procedure for analysis of HCCI combustion has been developed [15-17]. The procedure uses a two-step approach. Geometry-related information about the engine combustion chamber, specifically the temperature distribution within the cylinder as a function of time, is calculated by a computational fluid mechanics code (KIVA3V [18]). This temperature history information is then passed to a multi-zone detailed chemical kinetics code (HCT; Hydrodynamics, Chemistry and Transport, [19]). This procedure provides the benefits of linking the fluid mechanics and the chemical kinetics with a great reduction in the computational effort, to a level that can be handled with current computers.

In this model, HCT operates as multiple fixed-mass reactors with geometry-independent zones. The zones function to discretize the temperature distribution to providing a means of representing temperature gradients within the chemical kinetics simulation. In previous work 10 temperature zones have been used. The volume of these zones can change, but no mass transfer occurs at the zone boundaries. The total volume within the cylinder is a known function of time, as given by the slider-crank formula [20]. Knowing the total volume within the cylinder, the individual zone volumes are determined by applying an energy balance and equation of state (ideal gas law) to the individual zones and the cylinder contents as a whole.

The following procedure is used to conduct the simulations. First, KIVA3V is used to calculate the temperature distribution within the cylinder as a function of crank angle for

the compression stroke, with no chemical reactions considered. These temperatures within the cylinder are then discretized based on a specified zone mass distribution. HCT is then used to recalculate the compression stroke using temperature time histories supplied by KIVA3V. Once significant heat release occurs (2%), the KIVA3V temperatures are abandoned and the change in temperature for the fixed mass reactors are instead determined by an energy balance on the zone. After the transition from KIVA3V temperatures, the Woschni correlation is used to estimate heat transfer [21].

All of the previous work with this KIVA3V-HCT procedure has used 10 temperature zones for the chemical kinetics solver [15-17]. These 10-zone simulations have given accurate predictions of many performance parameters for HCCI engine combustion, such as indicated mean effective pressure, thermal efficiency, combustion efficiency, and burn duration. While previous work has shown that hydrocarbon emissions can be predicted with fairly good accuracy, typically within ±20% of experimental values, the multi-zone method has been shown to underpredict carbon monoxide (CO) emissions by an order of magnitude. Matching the conditions that result in formation of CO that does not react further to become carbon dioxide is difficult because the governing reactions are very sensitive to small changes in temperature (this is discussed further in the results section). Thus, greater resolution in temperature could improve the multi-zone model's capability to predict CO emissions in HCCI engines. This paper is focused on investigating the role of zone (i.e. temperature) resolution on the predictive capability of the multi-zone model, particularly with respect to hydrocarbon and CO emissions.

Results

The sensitivity of multi-zone model prediction of hydrocarbon and carbon monoxide emissions has been studied with respect to the number of zones used to discretize temperature. The simulations are compared to experimental data from isooctane HCCI combustion in a Cummins C engine with geometric and operating parameters as listed in Table 1. The base simulation case is a 10-zone simulation of isooctane HCCI combustion. Isooctane chemistry is handled with a detailed mechanism containing 859 species and 3606 reactions [22]. The mechanism does not currently include oxides of nitrogen (NO_x) formation chemistry. The authors realize that NO_x chemistry could have an impact on prediction of ignition timing [23], but in this case, this impact of neglecting NO_x chemistry is likely to be small because: (1) the concentrations of NO_x are very small because of low peak temperatures, and (2) the bottom dead center temperature can be adjusted slightly to compensate for the effect. The NO level at the start of the cycle for these experimental conditions is on the order of 0.05 ppm. Single-zone simulations with an isooctane mechanism that includes NOx chemistry (NOx chemistry as in Hori et al. [24]) show that there is little impact on the ignition timing with this initial NO level (combustion advances 0.05 crank angle degrees, equivalent to a bottom dead center temperature increase of 0.4 K). For engines with higher initial NO levels, NOx chemistry may play a more significant role in prediction of ignition timing.

The KIVA3V part of the simulation was conducted using an axisymmetric grid that had approximately 40,000 cells. Table 2 lists the division of mass between zones used for the 10-zone HCT simulation. Table 2 also lists the mass fractions for 20 and 40-zone

simulations of the same case. The mass fractions for the 20 and 40-zone simulations have been determined by evenly dividing the mass fractions from the 10-zone case by factors of two and four, respectively.

Figure 1 shows pressure traces for the experimental condition and the three simulations of this condition conducted using the zone mass fractions specified in table 2. The simulated and experimental traces agree very well. The most significant difference is that the 10-zone simulation shows a "stair-step" pressure rise during heat release while the 20 and 40-zone traces are much smoother - the pressure traces from the 20 and 40-zone simulations are essentially indistinguishable on the figure. The stair-step heat release is due to coarseness in the temperature discretization [25]; the ignition in each zone is temporally distinct in the 10-zone case, where the zone ignitions blend together better as the number of zones is increased. At top dead center the experimental pressure is about 2% greater than the KIVA3V predicted pressure trace. This small error is likely due to imperfections in the heat transfer prediction from the KIVA3V code. The rate of pressure rise in fig. 1 is more rapid for the experiment than for the simulation. The rate of heat release (and pressure rise) during combustion is governed by the interaction of the chemical kinetics with the temperature-time history distribution within the cylinder. Differences between the experiment and the KIVA3V prediction of these temperature-time histories could result in the discrepancy here. An additional possibility is the acoustic pressure oscillations apparent in the experimental results. We speculate that these pressure oscillations could result in local increases in temperature that would

accelerate the reaction rates. These pressure waves are currently not accounted for in the multi-zone model.

Quantitative results from the simulations and experiment are given in Table 3. The prediction of THC emissions by the multi-zone method is insensitive to whether 10 or more zones are used, but the predictions of CO emissions are very sensitive to zoning. The CO predicted at the end of the expansion stroke more than doubles for the 20-zone simulation relative to the 10-zone. Further refinement to 40 zones results in a slight drop in CO relative to the 20-zone case; the 40-zone simulation predicts nearly double the CO as the 10-zone simulation.

Figure 2 shows the zonal distribution in total hydrocarbon emissions at the end of the expansion stroke for the three different numbers of zones. The hydrocarbon emissions are normalized as a ratio of the mass of initial fuel carbon that is still present in hydrocarbon species at the end of the cycle relative to the initial fuel carbon mass. This normalization allows for direct comparison of results for simulations with different numbers of zones, where a value of 1 means that the hydrocarbon mass is equal to the initial fuel mass and a value of zero indicates that the fuel carbon has been completely converted to CO and carbon dioxide (CO_2). Values between zero and 1 indicate different fractions of conversion. The hydrocarbons are plotted versus the cumulative mass fraction for each zone. The cumulative mass fraction for a zone represents the sum of mass in the current zone and all previous (lower temperature) zones. For example, in the 10-zone case the first zone contains the first 2% of the mass, the second through fourth

zones each contain 1% of mass, the fifth zone contains the next 2% of the mass, and so forth. The cumulative mass fraction for the first zone is 0.02, the second zone 0.03, the third zone 0.04, and so forth. The highest temperature zone would have a cumulative mass fraction of unity. Fig. 2 shows that there is very little difference in the zonal distribution in hydrocarbons. Thus, the 10 zones initially used to discretize temperature are sufficient to consider the hydrocarbon prediction converged.

Figure 3 shows zonal CO at the end of the expansion stroke versus cumulative mass fraction. The relative CO emissions are the ratio of the mass of carbon in the carbon monoxide relative to the initial fuel carbon mass. A relative zonal fraction of unity would imply that all fuel carbon in a zone has been converted to CO with no further conversion to CO_2, while a value of zero would imply that no CO was created or all was converted to CO_2. The results for the different zone refinements are consistent up to a cumulative mass fraction of 0.045. The 10-zone model fails to resolve a significant CO contribution that occurs in neighboring zones. The 20 and 40-zone simulations show a large rise in CO at zones beyond a cumulative mass fraction of 0.045. 20 zones may still underresolve temperature; the mass fraction in the CO producing zones may still be too large, resulting in overprediction of CO relative to the 40-zone simulation. The 40-zone simulation yields better definition of the peak in CO, showing a sharp rise and then drop-off in the higher-temperature neighboring zone. This behavior explains the rise and fall of total CO as the number of zones is increased seen in fig. 3. For this case, 40 zones appears be sufficient to consider the CO prediction converged.

The 40-zone simulation is a "converged" solution, but still underpredicts the CO by a factor of 6 relative to the experiment. A variety of factors could play a role in the underprediction of CO. CO is very sensitive to small temperature changes within the cylinder and thus the implementation of heat transfer could significantly affect the prediction, particularly for the part of the cycle where the empirical correlation is used. During this part of the cycle the actual distribution in heat transfer from the zones is unknown and is specified ad hoc. The overall predictive capability of the method seems relatively insensitive to the use of the correlation, but prediction of a highly temperature sensitive process such as CO formation could be greatly affected. Neglecting mixing could also influence the results. Partially reacted or unreacted mixture in the crevices and boundary layer when the piston is at top dead center could mix with the hot core gasses during expansion. Hydrocarbons could be reacted to form CO and CO_2. Residual CO from the boundary layer could be converted to CO_2 due to the mixing.

The 40-zone simulation predictions of hydrocarbon and CO emissions at the end of expansion are shown in fig. 4. The relative fraction on the ordinate axis is the mass of carbon in the final zonal quantities of fuel, total hydrocarbons, and total hydrocarbons plus CO each divided by the initial zonal mass of carbon in the fuel. Fig. 4 shows that fuel in the first 2% (cumulative mass fraction of 0.02) does not react significantly. For cumulative mass fraction between 0.02 and 0.055 within the cylinder, roughly 40% of the fuel is unreacted, 30% of the fuel is converted to intermediate hydrocarbons, 20% of the fuel is converted to CO, and the balance is converted to CO_2. Hydrocarbons become essentially zero beyond a cumulative mass fraction of 0.055. In the next 0.25% of the

charge mass (cumulative mass fraction from 0.055 to 0.0575) 70% of the fuel is converted to CO and the balance is CO_2. In the next 0.0025, cumulative mass fraction ranging from 0.0575 to 0.06, about 15% of the fuel is converted to CO and the balance is CO_2. Beyond 6% of the charge mass (cumulative mass fraction of 0.06) essentially all fuel carbon is converted to CO_2. Four regions representing different degrees of completeness of combustion are present: an unburned fuel region; a partial conversion of fuel region containing unburned fuel, intermediate hydrocarbons, CO, and CO_2; a region where all hydrocarbons are converted to CO and CO_2, and a complete combustion region. These regions are labeled on fig. 4.

The species histories of fuel, CO and hydroxyl (OH) radicals provide insight into the processes occurring in these regions. Fig. 5 plots temperature versus crank angle and species versus crank angle for zones 16, 17, and 20 of the 40-zone simulation. Zone 16 (cumulative mass fraction of 0.475 to 0.5) is representative of the region that contains unburned fuel, intermediate hydrocarbons, and CO at the end of the expansion stroke. In zone 17 (cumulative mass fraction of 0.5 to 0.55) all fuel is consumed, but CO remains at the end of expansion. Zone 20 (cumulative mass fraction of 0.65 to 0.7) represents complete combustion. The temperature versus time history plot shows that there are very slight differences in temperature between these zones up to the start of combustion (start of combustion occurs at about 4° after top dead center), but these small differences are significant enough to produce dramatically different temperatures after combustion initiates. Achieving various levels of completeness of combustion is related to the balance between fuel, CO, and OH radicals. In zone 16, the fuel begins to react as the

OH radical population increases, but the OH is depleted with fuel still remaining. The fuel and CO in this zone do not react further once the OH radical is depleted. In zone 17 the population of fuel is entirely consumed. When fuel is no longer present the OH radical population rapidly increases and then begins attacking the CO. Once the OH radicals are consumed (and further production is halted), the CO within the zone becomes constant. In zone 20 the OH radical population is sufficient to rapidly consume fuel followed by rapid conversion of CO. A significant population of OH radicals remains when all CO is consumed; the remaining radicals recombine during the expansion stroke.

The production of the OH radicals in HCCI type engine conditions is triggered by the decomposition of hydrogen peroxide (H_2O_2) into two OH radicals [15], a highly temperature dependent chain branching reaction. Once the OH attack on CO begins the H_2O_2 decomposition chain branching reaction can be accelerated due to heat release that comes from conversion of CO to CO_2. The results shown in fig. 5 also suggest that mixing may not be negligible during expansion (again, mixing is not considered in the model). For example, in zone 20, a significant population of OH radicals remains for 40 degrees after all fuel and CO are reacted completely; sufficient time may be available for diffusion of reactive species into and out of neighboring zones, which would affect the final prediction of emissions.

Figure 6 shows the spatial location of the zones that encompass these regions at the time in the 40-zone simulation when the piston is at top dead center. The figure shows that most of the fuel in the crevice goes unburned. Zones that contain unburned fuel,

intermediate hydrocarbons, and CO at the end of expansion are found in the upper crevice, in the squish region, and at the corner of the bowl. The squish region is cooler due to convective heat transfer as the mixture is squeezed into the center of the combustion chamber during compression. Similarly, convective heat transfer cools the rounded corner of the bowl, as the flow tends to accelerate at the corner. The cooler temperatures in these regions result in the partial oxidation of fuel. The CO region is a very thin layer between the region containing fuel, intermediate hydrocarbons, and CO and the complete combustion region.

Conclusions

1. Increased zone resolution has little effect on prediction of overall performance (pressure traces, indicated mean effective pressure, thermal efficiency, combustion efficiency, burn duration).
2. Simulated pressure traces become smoother as more zones are used to discretize temperature.
3. Hydrocarbon emissions are relatively insensitive to increasing the number of temperature zones. For this case the 10-zone simulation was sufficient to consider the hydrocarbon prediction converged.
4. Prediction of CO emissions is very sensitive to the number of zones used in the simulation. The 20 and 40-zone simulations predicted roughly double the CO as the 10-zone run. The 40-zone simulation appears to sufficiently resolve the temperature within the cylinder so that the prediction of CO can be considered converged.

5. Even though the predicted CO appears to have converged with finer temperature resolution, the multi-zone method still underpredicts CO by a factor of 6. This may be due to simplifications in the model like neglecting expansion stroke mixing or limitations of the empirical heat transfer correlation used during combustion and expansion.
6. The completeness of combustion predicted by the model can be tied to production of hydroxyl radical within a particular zone.
7. The simulations indicate that most of the hydrocarbon and CO emissions come from the crevice and boundary layer in the squish region. Most of the mixture in the crevice remains unreacted. A partially oxidized mixture, which results in emissions of unburned fuel, intermediate hydrocarbons, and CO, is found to evolve from the upper part of the crevice and in the squish region boundary layer.

Acknowledgments
This project is funded by DOE, Office of Transportation Technologies, Steve Goguen and Gurpreet Singh, program managers. Work performed under the auspices of the U.S. Department of Energy by Lawrence Livermore National Laboratory under Contract W-7405-ENG-48.

References

1. Christensen, M. and Johansson, B., SAE Paper 982454.
2. Christensen, M., Johansson, B., Amneus, P., and Mauss, F., SAE Paper 980787.
3. Au, M., Girard, J.W., Dibble, R., Seibel, C., Maas, U., Aceves, S., Flowers, D., Martinez, J., and Smith, R., SAE Paper 2001-01-1894.
4. Flowers, D., Aceves, S., Smith, J.R., Torres, J., Girard, J., and Dibble, R., SAE Paper 2000-01-0328.
5. Flowers, D.L., Aceves, S.M., Martinez-Frias, J., Smith, J.R., Au, M.Y., Girard, J.W., and Dibble, R.W., SAE Paper 2001-01-1895.
6. Flowers, D.L., Aceves, S.M., Westbrook, C.K., Smith, J.R., and Dibble, R.W., *ASME J. of Eng. Gas Turb. Power* 123:433-439 (2001).
7. *Homogeneous Charge Compression Ignition (HCCI) Combustion, SP-1623*, Society Of Automotive Engineers, Warrendale, PA, 2001.
8. *HCCI Combustion, SP-1627*, Society of Automotive Engineers, Warrendale, PA, 2001.

9. *HCCI Technologies, SP-1642*, Society of Automotive Engineers, Warrendale, PA, 2001.
10. Noguchi, M., Tanaka, Y., Tanaka, T., and Takeuchi, Y., SAE Paper 790840.
11. Richhter, M., Alden, M., Hultqvist, A., and Johansson, B., SAE Paper 1999-01-3649.
12. Hultqvist, A., Christensen, M., Johansson, B., Franke, A., Richhter, M., and Alden, M., SAE Paper 1999-01-3680.
13. Onishi, S., Jo, S.H., Shoda, K., Jo, P.D., and Kato, S., SAE Paper 790501.
14. Hultqvist, A., Christensen, M., Johansson, B., Richhter, M., Nygren, J., Hult, J., and AldJn, M., SAE Paper 2002-01-0424.
15. Aceves, S.M., Flowers, D.L., Westbrook, C.K., Smith, J.R., Dibble, R.W., Pitz, W.J., Christensen, M., and Johansson, B., SAE paper 2000-01-0327.
16. Aceves, S.M., Martinez-Frias, J., Flowers, D.L., Smith, J.R., Dibble, R.W., Wright, J.F., and Hessel, R.P., SAE Paper 2001-01-3612.
17. Aceves, S.M., Flowers, D.L., Martinez-Frias, J., Smith, J.R., Westbrook, C.K., Pitz, W.J., and Dibble, R.W., SAE Paper 2001-01-1027.
18. Amsden, A.A., Los Alamos National Laboratory Report LA-13313-MS.
19. Lund, C.M., Lawrence Livermore National Laboratory report UCRL-52504.
20. Heywood, J.B., *Internal Combustion Engine Fundamentals*, McGraw-Hill Inc., New York, 1988.
21. Woschni, G., SAE Paper 670931.
22. Curran, H.J., Gaffuri, P., Pitz, W.J., Westbrook, C.K., and Leppard, W.R., SAE Paper 952406.
23. Eng, J.A., Leppard, W.R., Najt, P.M., and Dryer, F.L., SAE Paper 972889.
24. Hori, M., Matsunga, N., Marinov, N., Pitz, W., and Westbrook, C., Proc. Comb. Inst. 27:389-396 (1998).
25. Andreatta, D., Ph.D Dissertation, University of California, Berkeley, 1995.

This work was performed under the auspices of the U.S. Department of Energy by the University of California, Lawrence Livermore National Laboratory under Contract No. W-7405-Eng-48.

Table 1 - Main characteristics of the Cummins C single cylinder engine and specific test conditions used for comparison.

Engine Parameters	
Displaced volume, cm^3	1378
Bore, mm	114
Stroke, mm	135
Connecting rod length, mm	216
Geometric compression ratio	10.5:1
Swirl ratio	3.6
Exhaust valve open (degrees ATDC)	135
Exhaust valve close (degrees ATDC)	370
Intake valve open (degrees ATDC)	350
Intake valve close (degrees ATDC)	574
Geometry	Cylindrical bowl-in-piston
Test Conditions	
Engine speed, rpm	2007
Intake temperature, K	413
Absolute intake pressure, bar	3.11
Equivalence ratio	0.348

Table 2 - Zone mass fractions for the three zone resolutions simulated. The zone number is for the 10-zone case. For the 20-zone and 40-zone cases the masses in each zone are divided into two and four equal portions.

Zone Number	**Mass fraction in zone**		
	10-Zone	20-Zone	40-Zone
1	0.02	0.010×2	0.0050×4
2	0.01	0.005×2	0.0025×4
3	0.01	0.005×2	0.0025×4
4	0.01	0.005×2	0.0025×4
5	0.02	0.010×2	0.0050×4
6	0.05	0.025×2	0.0125×4
7	0.10	0.050×2	0.0250×4
8	0.18	0.090×2	0.0450×4
9	0.25	0.125×2	0.0625×4
10	0.35	0.175×2	0.0875×4

Table 3 - Main HCCI combustion characteristics of the two cases selected for analysis.

	Experiment	10-Zone	20-Zone	40-Zone
Peak cylinder pressure, bar	112.4	110.8	110.6	110.7
CAD for peak heat release (degrees ATDC)	7.0	7.0	7.0	7.0
Burn duration, CAD[a]	9.6	7.6	8.0	8.1
Combustion efficiency, %	96.1	96.1	96.0	96.1
Gross IMEP, bar	10.7	11.9	11.9	11.9
Gross indicated efficiency, %	43.4	48.0	48.0	48.0
HC emissions, g/kg fuel	32.0	42.3	42.3	42.4
CO emissions, g/kg fuel	31.5	2.8	6.0	4.9
NO_x emissions, g/kg fuel[b]	0.228	-	-	-
NO_x emissions, ppm[b]	5.28	-	-	-

a. Burn duration is defined as the crank angle between the two points at which apparent heat release is 10% of the peak heat release.

b. Oxides of nitrogen (NO_x) formation chemistry are not included in the kinetic mechanism used, so no simulation results are available

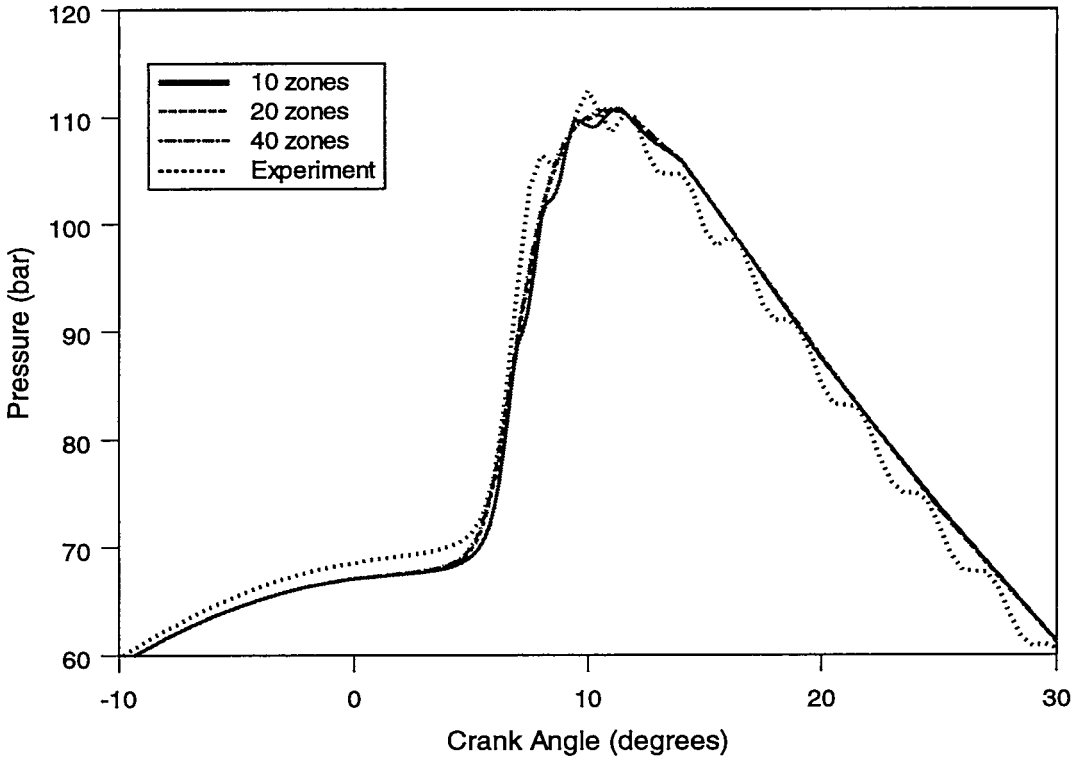

Fig. 1 – Pressure trace comparison between the three simulation cases and the experiment.

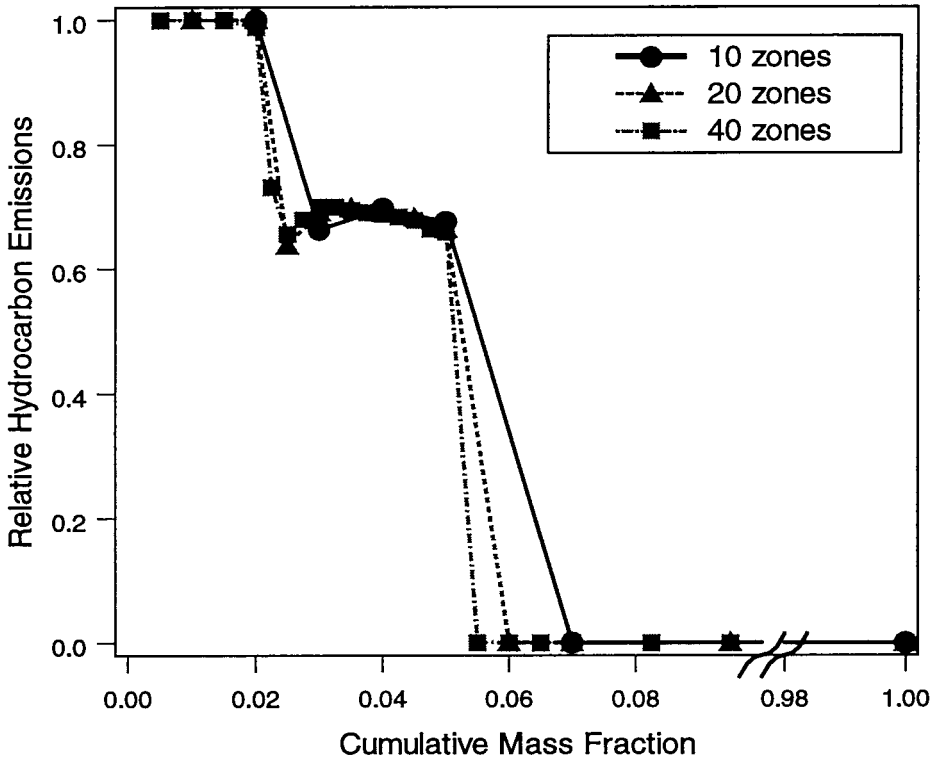

Fig. 2 – Zonal distribution of total hydrocarbon emissions for the three simulation cases. The relative emissions are defined as a mass fraction of initial fuel carbon that is present at the end of the cycle as a hydrocarbon species (either unburned fuel or intermediate hydrocarbon species) divided by the initial mass of fuel carbon. This normalization allows for direct comparison of simulations with different numbers of zones. Note that the axis is broken at a cumulative mass fraction of 0.1 – emissions are constant (zero) to cumulative mass fraction of unity.

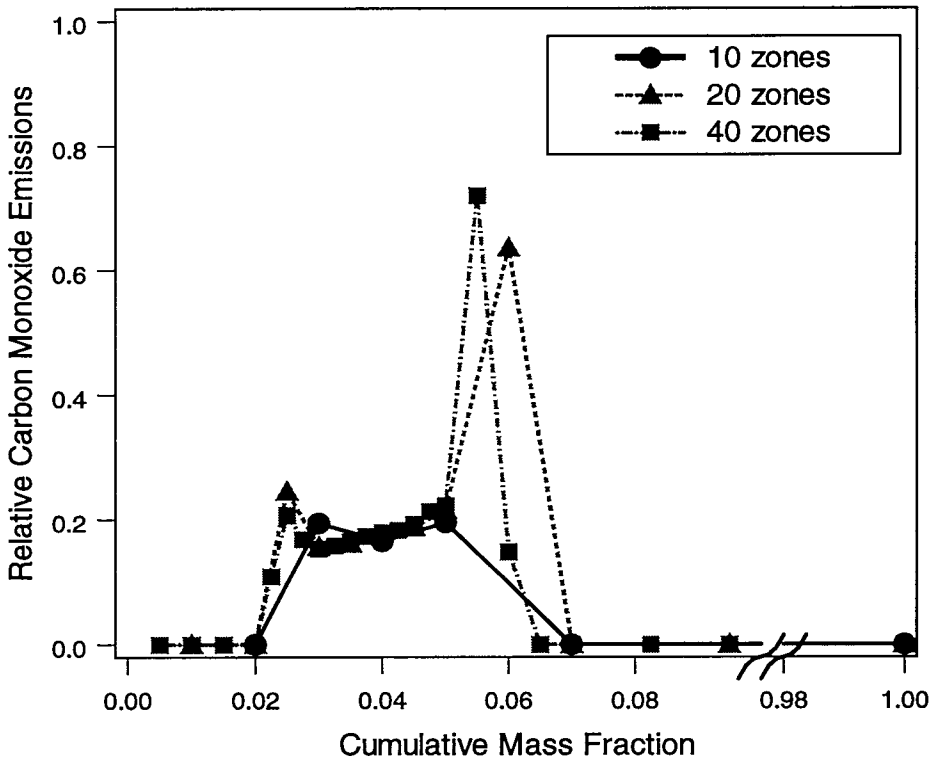

Fig. 3 – Zonal distribution of carbon monoxide emissions for the three simulation cases. The relative emissions are defined as a mass fraction of initial fuel carbon that is present at the end of the cycle as a carbon monoxide species divided by the initial mass of fuel carbon.

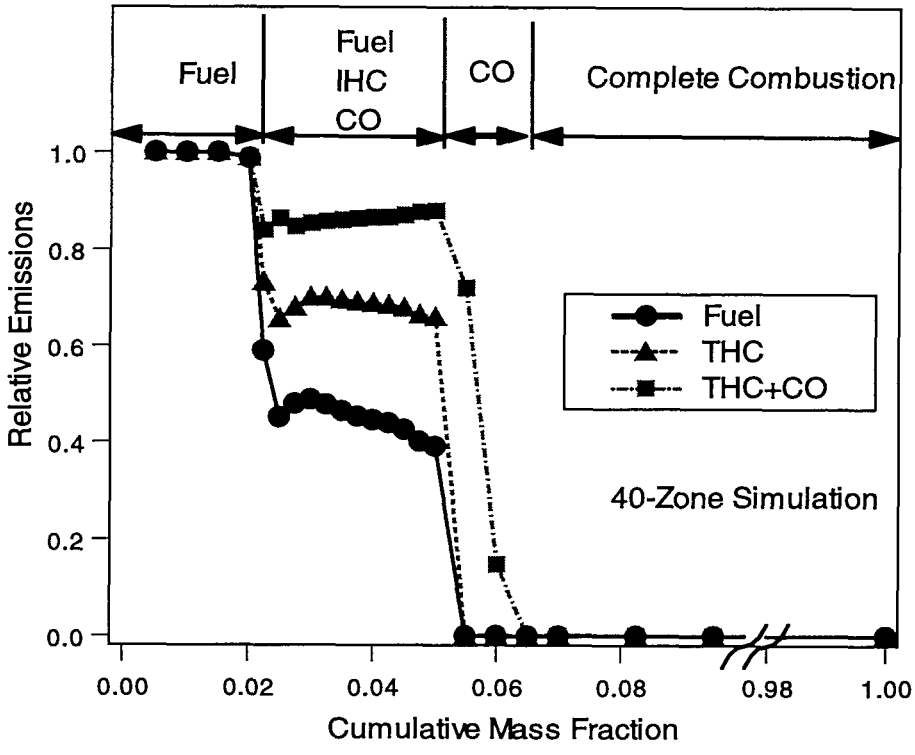

Fig. 4 – Zonal distribution of relative fuel, total hydrocarbon, and carbon monoxide emissions for the 40-zone simulation. The relative emissions are defined as a mass fraction of initial fuel carbon that is present at the end of the cycle as a fuel, fuel plus intermediate hydrocarbons (THC), and fuel plus intermediate hydrocarbons plus carbon monoxide species (THC+CO), respectively, divided by the initial mass of fuel carbon. Regions in the cumulative mass fraction that produce emissions of unburned fuel, unburned fuel plus intermediate hydrocarbons (IHC) plus carbon monoxide (CO), and carbon monoxide are labeled.

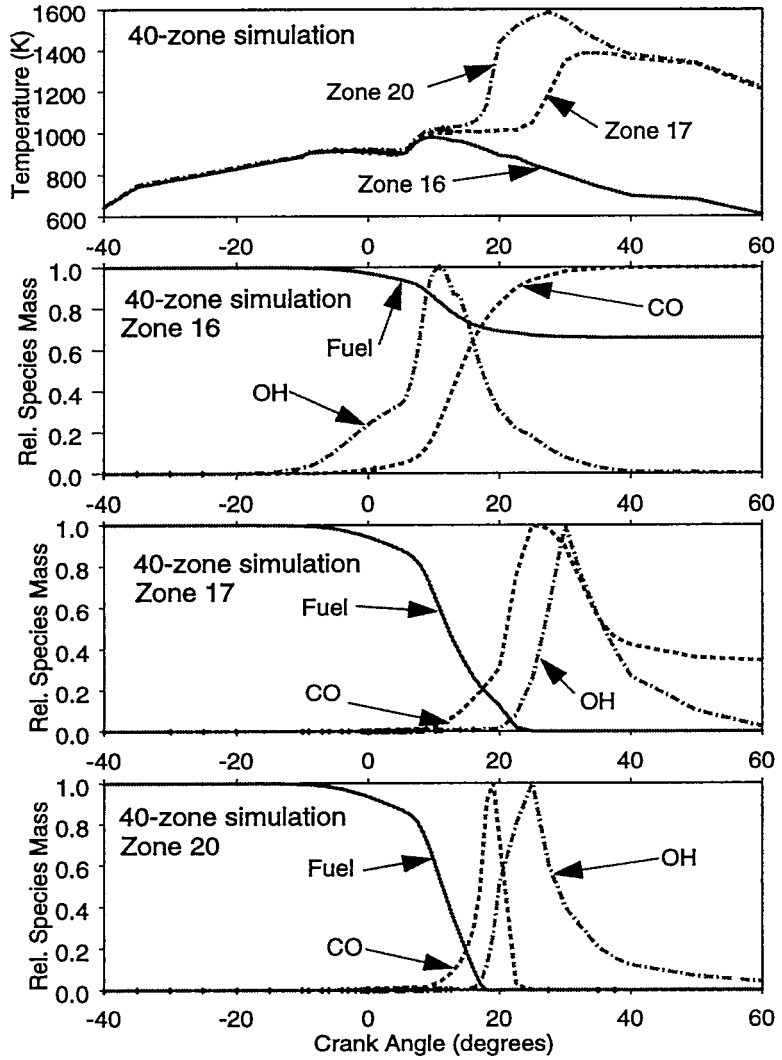

Fig. 5 – This figure shows fuel, carbon monoxide (CO), and hydroxyl (OH) radical mass fractions plotted versus crank angle for zones 16, 17, and 20 from the 40-zone simulation. The species mass is normalized in each figure by the maximum species mass in that zone during the engine cycle. Also shown is temperature versus crank angle for each of these zones. Zone 16 is representative of the region that results in a mixture of fuel, intermediate hydrocarbons, and carbon monoxide at the end of the cycle. Zone 17 has no fuel remaining at the end of the cycle, but has unconverted carbon monoxide at the end of the engine cycle. Zone 20 undergoes complete combustion.

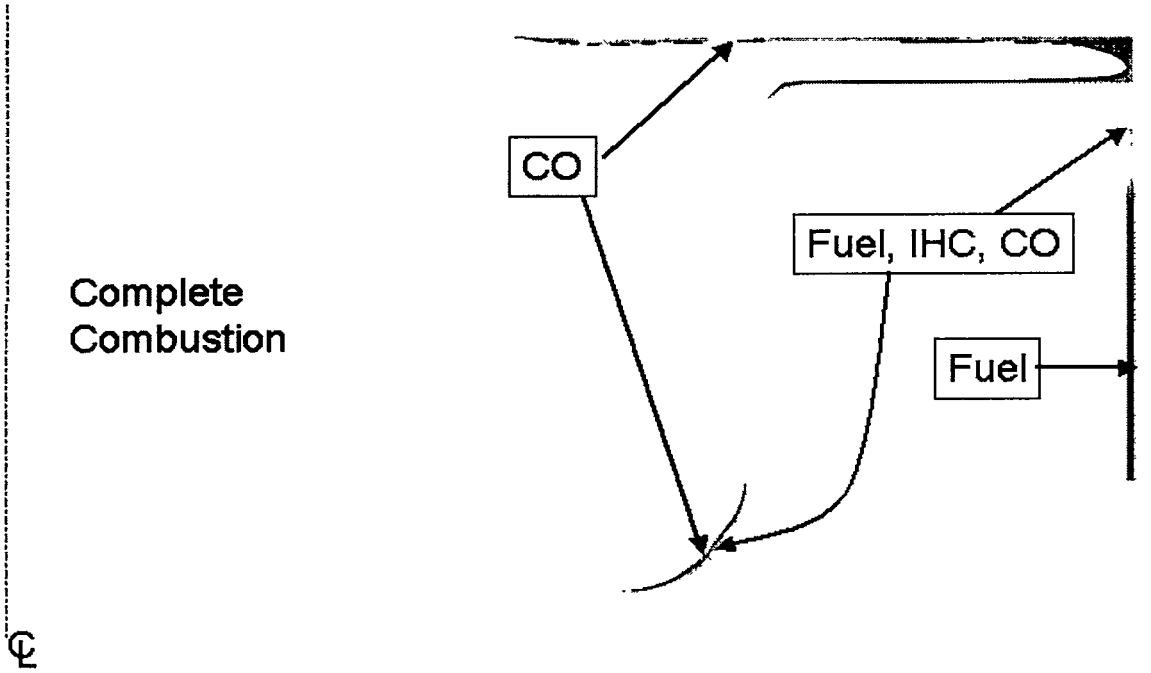

Fig. 6 – Visualization of the spatial locations within the combustion chamber where emissions are produced. The figure shows an axisymmetric slice of the combustion chamber at top dead center. The location of zones that are found to be the source of unburned fuel, unburned fuel plus intermediate hydrocarbons (IHC) plus carbon monoxide (CO), and carbon monoxide emissions at the end of the expansion stroke are labeled. Also shown is the region of complete combustion.